Machine Learning to Empower Electrohydrodynamic Processing

Fanjin Wang[1], Moe Elbadawi[1], Scheilly Liu Tsilova[1], Simon Gaisford[1], Abdul W. Basit[1], Maryam Parhizkar[1*]

[1]Department of Pharmaceutics, UCL School of Pharmacy, University College London, 29-39 Brunswick Square, London WC1N 1AX, UK.

[*] Corresponding author: Parhizkar, Maryam (m.parhizkar@ucl.ac.uk).

Abstract

Electrohydrodynamic (EHD) processes are promising healthcare fabrication technologies, as evidenced by the number of commercialised and food-and-drug administration (FDA)-approved products produced by these processes. Their ability to produce both rapidly and precisely nano-sized products provides them with a unique set of qualities that cannot be matched by other fabrication technologies. Consequently, this has stimulated the development of EHD processing to tackle other healthcare challenges. However, as with most technologies, time and resources will be needed to realise fully the potential EHD processes can offer. To address this bottleneck, researchers are adopting machine learning (ML), a subset of artificial intelligence, into their workflow. ML has already made ground-breaking advancements in the healthcare sector, and it is anticipated to do the same in the materials domain. Presently, the application of ML in fabrication technologies lags behind other sectors. To that end, this review showcases the progress made by ML for EHD workflows, demonstrating how the latter can benefit greatly from the former. In addition, we provide an introduction to the ML pipeline, to help encourage the use of ML for other EHD researchers. As discussed, the merger of ML with EHD has the potential to expedite novel discoveries and to automate the EHD workflow.

Keywords: 3D printing drug products; Continuous Manufacturing; Nanotechnology; Digital Healthcare Technology; Informatics; Functional Materials; 2D materials.

Precise, Rapid, and Timely

Electrohydrodynamic (EHD) processes are a collection of *state-of-the-art* fabrication techniques that are capable of generating structural features in the order of micron to nano-size [1, 2]. EHD techniques have been used to fabricate nanofibers, nanoribbons, and spherical nanoparticles [3-7]. The technology leverages voltage-control for high precision fabrication in a reproducible manner [8]. Moreover, the standard EHD setup is simple, inexpensive and compact. As it is a solvent-based fabrication technique and does not require high heat, a wide range of polymers can be used. However, in contrast to other solvent-based techniques, the drying times are considerably fast, making it a uniquely rapid-fabrication process. In addition, as high temperature is not required, biological and thermally-labile materials can be incorporated, as well as hybridised products containing ceramics and metals [1, 9]. Furthermore, highly porous structures, up to 90% porosity, can be obtained yielding high surface area-to-volume ratio, which is a requirement for certain applications [3, 10, 11]. These aforementioned remarkable properties of EHD highlight why the technology is employed across a number of sectors, including drug delivery, tissue engineering, sensors and energy harvesting [12, 13]. With its broad application and several EHD products successfully progressed towards clinical or industrial application (**Table 1**), the technology warrants further research.

One promising research is the transition from two- to three-dimensional printing (3DP) EHD processes. For example, EHD can achieve features on a scale magnitude smaller than that of current 3DP technologies, resulting in highly sensitive biosensor electrodes. Moreover, the morphology of some products has been found to replicate the extracellular matrix that facilitates biocompatibility, and which current 3DP technology-based scaffolds are unable to. Hence, due to these specialised properties, 3DP-EHD technologies are expected to become a staple 3DP technology complimenting existing 3DP technologies [14].

The transition to a 3DP technology will undoubtedly require a period of optimisation in order to realise this aim. Recent research has revealed that 3DP technologies that are an extension of conventional 2D fabrication technologies were not always compatible with existing formulations. In addition, the conventional 2D-EHD processes are far from having their full potential realised. For one, large scale production are yet to be realised, despite the technology being around for decades. The technology is highly complex, with each parameter playing an important role and has interdependent influence on the characteristics of the particles or fibres produced. Of course, the ability of EHD to accommodate a wide range of materials is advantageous, however, it is inescapable that exploring the influence of each parameter will be laborious (**Table 2**). The currently used trial-and-error approach is antiquated and unsustainable, requiring large resources of materials and time. In addition, some healthcare applications of EHD, such as point-of-care wound dressing fabrication, will ideally need to be situated in healthcare facilities – nearer to the patient, on-demand and personalised. However, this will require on-site expertise, which can be costly for healthcare institutes.

Table 1. Examples of EHD products both food and drug administration (FDA) approved and in clinical trials.

Brand name	Manufacturer	Product	Material	Approval	References
SurgiCLOT	St Theresa Medical	Bone healing	Dextran nanofibers	Clinical Use	(St Teresa Medical, 2021)
PK Papyrus	Biotronik	Coronary stent system	Polyurethane fibres	FDA	(Biotronik, n.d.)
Spincare	Nanomedic Technologies	Portable bedside wound-care device	Customised polymers	CE certified	(Nanomedic Technologies, 2020)
NanoCare	Nanofiber Solutions	ECM-like fibre structure for wound healing	FDA-approved polymers	FDA	(NanoFiber Solutions, 2021)
ReBOSSIS	ORTHOReBIRTH	Synthetic bone-filling	Cottony-type Bone-void filling material: β-Tricalcium Phosphate (β-TCP) Bioabsorbable Polymer Silicone-containing Calcium Carbonate (Si V)	FDA	(ORTHOReBIRTH, n.d.)
Rivelin Patch	AFYX Therapeutics	Patch drug delivery system to mucosal lining for Oral Lichen Planus	Patch containing clobetaso	Phase 2 Clinical trial Cleared	(AFYX Therapeutics, 2020)

Table 2. Processing parameters for EHD

Processing parameters	Flow rate
	Applied voltage
	Distance between nozzle and collection plate
	Needle/nozzle diameter
Solution parameters	Type of polymer
	Polymer solution concentration
	Drug carried and concentration
	Type of solvent
	Viscosity
	Surface tension
Ambient/environmental parameters	Temperature
	Humidity

To help expedite this process, modelling techniques have recently been incorporated to simulate the EHD process [15-18]. Such simulations help to reduce the exhaustive trial-and-error approach to obtaining data whilst minimising material consumption. The state-of-the-art in modelling is Machine learning (ML), a subset of artificial intelligence (AI) that is strongly implicated in the next healthcare revolution [19-21]. ML is the process of developing algorithms to learn from data and help develop predictive models therefrom [22, 23]. ML is a widely versatile predictive technique, capable of making predictions from a variety of inputs, including numeric, text, images and videos. In addition, the predictions can be made in a matter of seconds, making it suitable for time-sensitive applications, such as in healthcare [24]. The recent application of deep learning, a subset of ML, has demonstrated that algorithms can be developed that improve their predictions as the data size grows, having previously considered 'Big data' to be an obstacle in ML. Due to these outstanding and unprecedented properties, the success of both AI and ML has garnered much attention, with well-publicised success stories such as AlphaGo and AlphaFold, and some algorithms have outperformed clinicians in diagnostic tests [25-27]. As a consequence, a number of research disciplines have incorporated ML, chief among them the drug discovery discipline [28] and other healthcare-related applications (**Table *3***). However, the adoption of ML in the wider material science and engineering field has not been thoroughly explored, even though the field is heavily data-driven. Hence, given the large existing available data, there is potential to employ ML in material science to help expedite research and development.

To that end, the current paper reviews the application of ML applied in EHD processes, the principal objective being to introduce ML to the EHD community. A section providing essential background to ML is presented first, highlighting the examples of common ML techniques (MLT) and their learning methods, as well as describing the overall ML pipeline itself. The following section summarises the application of ML in EHD, before concluding the paper by providing a perspective on the outlook on this emerging multidisciplinary field.

Table 3. A number of Machine Learning Algorithms are being investigated for clinical use.

Algorithm	Clinical Application	Ref
Random Forest	Clinical Trial design	[29]
Artificial Neural Networks	Powering Exoskeletons	[30]
Convolutional Neural Networks	Image recognition software	[31]
Principal Component Analysis	diagnostic	[32]
k-means	diagnostic	[32]
Support Vector Machine	Diagnostics	[33]
Recurrent Neural Networks	Diagnostics	[34]
Gaussian Mixture Model	Imaging	[35]

Machine Learning Principles

ML focuses on algorithms that train prediction- or decision-making models based on data provided [36].The exponential increase of computational power and the advancement of ML algorithms have enormously accelerated the application of ML in a myriad of fields not limited to computer science but also biology [25], chemistry [37], materials science [38, 39], and pharmaceutical science [40-43]. On top of applications in academia, ML is also having a huge impact on industries, of which facial recognition, text translation, and self-driving cars are classic examples [44-46]. ML encompasses several categories of learning methods. Depending on the information the training data contains, ML can be divided into two major categories of supervised learning and unsupervised learning [47, 48]. These algorithms are discussed in detail in the following section.

Supervised learning

Supervised learning is a popular and widely used method in ML [48]. During the training process, the data are fed into the learning algorithm f in the form of $(feature, label)$ pairs. Taking linear regression as an example, dots that contain (x, y) positions are the $(feature, label)$ pairs in the training step. Training with (x, y) pairs allows the regression algorithm f_{reg} to build up a model that gives a prediction of $\hat{y}$ with a query input x. Other than numeric (x, y) input, the input features can also be medical images, molecular graphs, or texts (DNA sequence or simplified molecular-input line-entry system (SMILES)) in different algorithms [49-51]. **Table *4*** shows different learning algorithms in supervised learning to which the well-known multiple linear regression, support vector classification (SVC), and multilayer perceptron (MLP) belong.

An illustration of several ML techniques is shown in **Figure *1***. Briefly, multiple linear regression (MLR) learns a linear combination of features $\hat{\boldsymbol{y}} = \boldsymbol{\theta}^{\boldsymbol{T}}\boldsymbol{x} + b$ that minimizes the squared error of the predicted value to the ground truth value. Similarly, logistic regression (LR) uses a linear combination of features $\boldsymbol{\theta}^{\boldsymbol{T}}\boldsymbol{x} + b$ but then takes the combined result and feeds it into a logistic

function to do classification tasks. *k*-Nearest neighbours (kNN) algorithm approaches classification by a simple plurality vote of *k* nearest neighbours. The label of the predicting sample will be assigned to the most common class amongst its neighbours. Support vector classification seeks the hyperplane $\boldsymbol{\theta}^{\boldsymbol{T}}\boldsymbol{x} + b = 0$ that separates samples of different categories the most. Moreover, non-linear classification can be performed by SVC with the help of kernel methods [52]. Naïve Bayes algorithm adopts the Bayes' theorem to calculate the posterior probability of the predicting sample's label based on prior known samples in the training step [36]. Decision tree (DT) uses a series of simple rules (e.g., comparing with criteria) to predict [53]. Random forest (RF) uses an ensemble learning method 'bagging' which combines the prediction results from many different decision trees and gives a final prediction by a majority vote in classification or averaging the output in regression [54]. Also based on DT, gradient boost decision tree (GBDT) belongs to the 'boosting' ensemble learning method. GBDT takes the output of one decision tree and feed it to another decision tree, forming a series connection of models [55]. MLP is a basic structure of artificial neural networks (ANN) consisting of multiple layers of neurons [56]. Here we adopt a broader definition of MLP where the activation function is not limited to the threshold function. A classic structure of MLP consists the input layer, hidden layer(s), and the output layer. These layers are connected by activation functions like rectified linear function (ReLU), sigmoid function, or tanh function. Backpropagation (BP) trains parameters in the MLP network, minimizing the loss function. Because of the non-linear nature of the activation functions, MLP performs well in capturing non-linear relationships between the features and the labels [57]. Supervised convolutional neural networks (CNN) and recurrent neural networks (RNN) are specialized neural networks designed to handle image and serial (e.g., texts and audio) inputs [44, 58, 59].

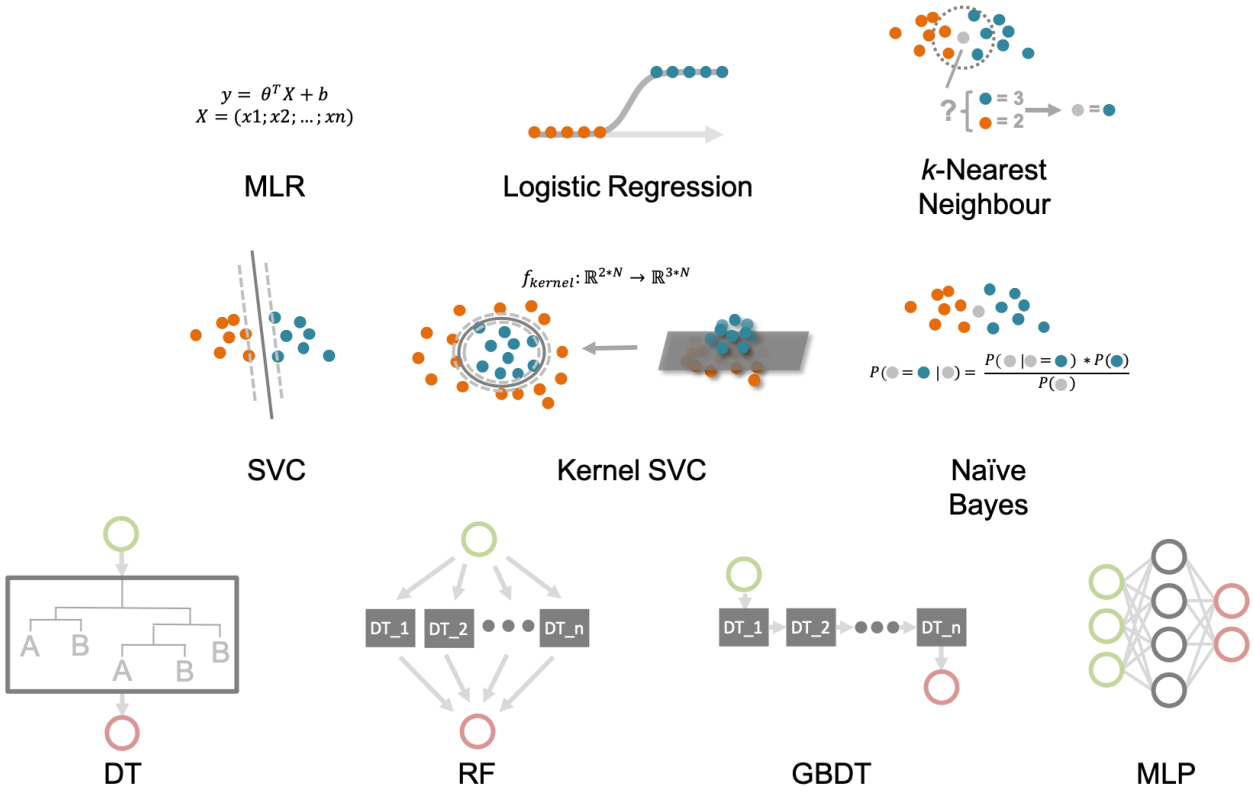

Figure 1. Schematic representation of frequently used supervised ML algorithms (MLR – multiple linear regression; LR – logistic regression; SVC – support vector classification; DT – decision tree; RF – random forest; GBDT – gradient boost decision tree; MLP – multi-layer perceptron). (y – response variable; $\theta^T x$ – denotes the input features; P- is probability; f_{kernel} – kernel function; $\mathbb{R}$ - real numbers; n - number).

Unsupervised learning

Unlike supervised learning, the input data of unsupervised learning algorithms are without labels [60]. Unsupervised learning algorithms are able to find the intrinsic patterns of data based on different assumptions [48]. Several unsupervised learning algorithms are shown in **Table *4***. Conventional unsupervised learning algorithms mainly tackle two tasks: clustering and dimensionality reduction [60]. **Figure 2** includes some unsupervised learning algorithms. *k*-means clustering algorithm partitions the data to *k* clusters by finding out the minimum in-cluster variance. Gaussian mixture model (GMM) assumes data are generated from several Gaussian distributions with unknown parameters and aims to find out the underlying distributions to cluster the data. Dimensionality reduction aims to address the 'curse of dimensionality', caused by the sparsity of data (i.e. not enough data to fill up the high-dimensional feature space to reach statistical significant conclusions), by detecting and removing the redundancy in features. Principal component analysis (PCA) finds a lower-dimensional representation by linearly transforming original data while maximizing the variance in the new sample space [61]. Recently,

novel unsupervised learning algorithms including variational autoencoder (VAE) and generative adversarial networks (GAN) target new data generation from the learned latent pattern of training data [62, 63]. In certain scenarios, pre-trained CNN and RNN are used for unsupervised feature extraction for image and text data.

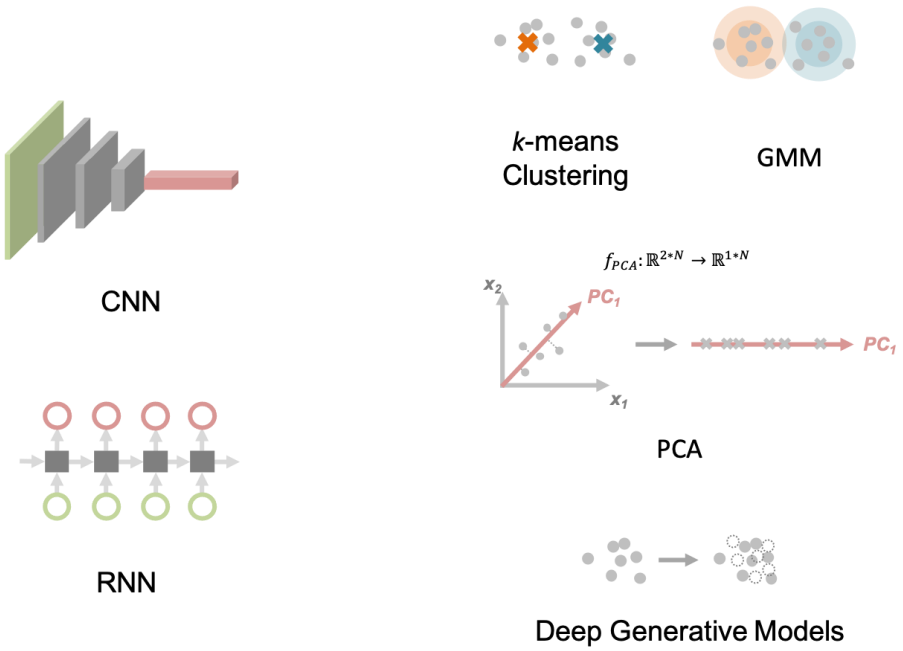

Figure 2. More schematic representation of ML algorithms commonly used (CNN – convolution neural network; RNN – recurrent neural network; GMM – gaussian mixture model; PCA – principal component analysis). (f_{pca} – PCA function; $\mathbb{R}$ - real numbers; n – number).

Table 4. Machine Learning Algorithms

ML Algorithms	Category	Description	Applications	Ref
		Linear models		
Multiple Linear Regression	Supervised, Regression	Correlate multiple input features to the targeting label by a linear regression model	Structural-properties relationship models	[64, 65]
Logistic Regression	Supervised, Classification	Using logistic function to do binary classification	Classification models, feature importance analysis	[66, 67]
		Tree-based Ensemble Learning		

Random Forests	Supervised, Classification or Regression	A bagging ensemble learning algorithm	Structural-properties relationship models, classification models	[68, 69]
Gradient Boosting Decision Tree	Supervised, Classification or Regression	A boosting ensemble learning algorithm	Structural-properties relationship models	[70, 71]
		Neural Networks		
Multilayer Perceptron	Supervised, Classification or Regression	A type of simple artificial neural network with a few hidden layers	Structural-properties relationship models, classification models, materials design	[72-74]
Recurrent Neural Networks	Supervised or Unsupervised	A type of neural networks with recurrent units, specialized in handling sequential data	Translation, text information extraction, retrosynthesis analysis	[37, 39, 44]
Convolutional Neural Networks	Supervised or Unsupervised	A type of neural networks with convolutional layers, specialized in handling image data	Image information extraction, molecular featurization	[58, 75, 76]
		Other		
Support Vector Machine	Supervised or Unsupervised	An algorithm usually combined with kernel method to seek for decision boundaries	Structural-properties relationship models, classification models, materials design	[77-79]
k-Nearest Neighbours	Supervised, Classification or Regression	A simple algorithm based on plurality votes or the	Structural-properties relationship models,	[80, 81]

		average value of k nearest neighbours	classification models	
Naïve Bayes	Supervised, Classification	An algorithm using Bayes' theorem to classify data with an assumption of naïve independence between data features	Classification models	[82]
k-means Clustering	Unsupervised, Clustering	A clustering algorithm assuming data come from k clusters	Exploring inner relationships within data	[83, 84]
Gaussian Mixture Model	Unsupervised, Clustering	A clustering algorithm assuming data come from different gaussian distributions	Exploring inner relationships within data	[84, 85]
Principal Component Analysis	Unsupervised, Dimensionality Reduction	A dimensionality reduction algorithm to linearly reduce data dimension	Small dataset training, dimensionality reduction	[86, 87]
Deep Generative Models	Unsupervised, Generative	A subset of algorithms with the ability to generate new data from the same statistical distribution as the given data	Molecular design, material design	[88-90]

Feature Engineering

Feature engineering includes processing raw data to computer-understandable data and the refinement of extracted features [91]. Most of the time, unprocessed raw data will dramatically limit, if not completely hinder, the performance of ML algorithms. Especially in materials science and chemistry, crystal and molecular information is represented by a chemical formula or a molecular graph which can be easily understood and interpreted by human experts. However, such information is not sufficient nor valid as the input of ML algorithms like multiple linear regression. Hence, appropriate feature engineering should be carried out on the raw data. For organic molecules and crystals, molecular fingerprints and crystal descriptors are introduced to enable computers to understand chemical and structural information [92, 93]. Apart from molecules, different data types usually require specific feature engineering techniques [91]. Numeric data need to be normalized or transformed into the logarithm scale. Image data need to be resized or cropped. Text data should be vectorized by featurization methods like bag-of-words. Regarding the refinement of extracted features, the number of features is the major concern. Furthermore, in feature engineering, some unsupervised learning algorithms like PCA are applied to rule out the redundancy in data [91, 94]. In short, feature engineering is the preparation of raw data and making it ready for the further training process. A summary of common feature engineering techniques is presented in **Table *5***.

Table 5 Summary of common Feature Engineering Techniques

Feature Engineering Techniques	**Input**	**Benefits**	**Ref**
Scaling, normalization, log-transform	Numerical	Speed up convergence, balance weight between features, prevent fast saturation of activation functions	[91]
Bag-of-Words, Word2Vec	Text	Embed words into vectors	[95]
Convolutional Neural Networks	Image	Extract edges and structural features in images	[58, 59]
Simplified molecular-input line-entry system (SMILES)	Molecules	Transfer molecular information into text expression	[96-98]
Morgan fingerprints, Mol2Vec, Molecular ACCess System (MACCS)	Molecules	Transfer molecular information into vector expression	[99-101]

Matminer, ElemNet	Inorganic Crystals	Describe inorganic materials with crystal information	[102, 103]

Model training and hyper-parameter tuning

As the parameters of EHD need to be optimized (**Table 2**, e.g. voltage, collector distance, etc.), so do the parameters for the ML algorithms. In most ML algorithms, hyper-parameters are available for further adjustment of the structure or learning behaviour of the model. For instance, in MLP, the number of neurons and hidden layers determine the complexity of the network, making them critical hyperparameters in the model which govern the overfitting or underfitting of the network [104]. Overfitting refers to the conditions where the network remembers all the training data, resulting in the training accuracy close to 100%. However, the overfitted model is not robust and yields weaker prediction accuracy in the following evaluation process. Hyper-parameters should be fine-tuned based on different training tasks to optimize the model performance. Common methods of hyper-parameter searching include random search, grid search, and Bayesian optimization [105]. These methods try out different hyper-parameters in a pre-set manner, compare the performance of each hyper-parameter set, and present the one with the best performance measured by user-determined performance metrics [106].

As the name suggests, random search explores the parameter space in a random manner, and selects the parameters that yielded the optimum prediction value (e.g. highest accuracy) [107]. Grid search, on the other hand, is more structured to tuning the parameters, where the user selects the range of parameters to examine. Taking neural network as an example, the user will request specific values of hidden layers to be examined [108].

Model Evaluation

Evaluating the model provides essential information about the performance. The data can be first divided into training/validation/test sets before training. Model performance on the test set is regarded as the performance of a model in real application scenarios. Sometimes validation and test sets are not distinguished, and the data will only be separated into training/test sets. The ratio of the training set to the test set is not fixed but is normally taken as 80/20 [42]. In datasets with limited data size, cross-validation (CV) is a useful technique performed to make full use of all data [109]. Multiple methods are available for CV [110]. By splitting the training set into k groups, $k-1$ groups are treated as the training set and the remaining one group is used as the validation set, as shown in **Figure 3(A)**. Then, model training and validation are performed k times so that all groups have been treated as the validation set. This technique is called k-fold CV. In extreme conditions where k equals to the sample size n such that one group only has one sample, the technique is referred to as leave-one-out CV (LOOCV). The overall performance of a model in CV is calculated by averaging the performance metrics over all rounds of CV [111, 112].

There is a wide range of metrics that are used [110]. For classification tasks, accuracy is the salient metric, which is the ratio of correct predictions to that of the total number of predictions. Other common metrics include sensitivity and specificity, which are common in medical diagnostics since it is pertinent to evaluate both the true positives and true negatives. An illustration of a few metrics applied in ML tasks is shown in **Figure 3(B)**. The matrix here between the predicted and ground truth value is known as the confusion matrix. In material science domain, researchers are mainly interested in the true positives (i.e. 'Does it work?'). For example, ML was applied to 3D printing where researchers were only interested in how well an algorithm was able to identify which formulations were printable, and less interested in how well the algorithm was able to identify which formulations were unprintable [24]. Here, the metrics precision and recall were applied. Precision evaluates how well an algorithm is able to identify the true positives from all that are predicted as positives. Taking the 3D printing study as an example, a precision of 80% resulted in 20% of formulations being predicted as printable which were in fact not printable. Moreover, the F1-score, calculated from the harmonic mean of precision, is widely used in classification tasks by taking both aspects into consideration. A valuable question in ML is how to establish a baseline value for classification tasks, such that the prediction of the ML algorithm is useful. Here, the Cohen's kappa (*k*), the Matthew's correlation coefficient (MCC), the receiver operating characteristic curve (ROC) and the area under the receiver operating characteristic curve (AUROC) have been employed. These metrics compare the performance of the ML algorithm to random prediction, where a value of 0 for Cohen's kappa and MCC and a value of 0.5 for AUROC indicates the ML performance to be the same as random prediction [113-115].

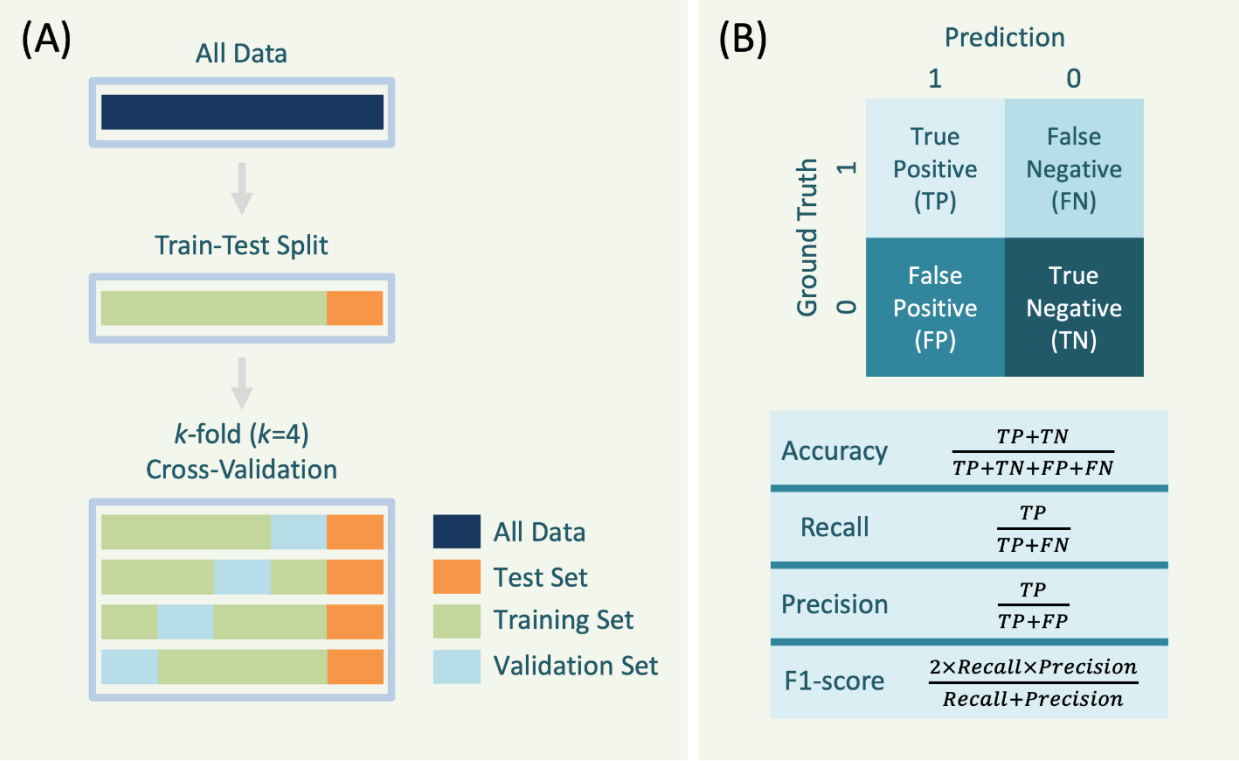

Figure 3 *(***A***)* Train-Test split and cross-validation step. **(B)** The confusion matrix and metrics used for evaluating ML model performance. (k – constant; TP – true positive; TN – true negative; FP – false positive; FN – false negative)

For regression tasks, the metrics aim to measure the difference between the predicted value $\hat{y}$ to the ground truth value y. A well-known and widely used metric is mean squared error (MSE), expressed as:

$$\frac{1}{n}\sum_{i}^{n}(y_i - \hat{y}_i)^2 \qquad \textbf{Equation 1}$$

(where *n* is the number of samples, *i* is the index and $\sum$ is the summation). For which the square root is sometimes taken, giving the root mean squared error (RMSE). The RMSE and MSE metrics are used extensively in linear regression scenarios to evaluate the performance of regression. Similarly, the mean absolute error (MAE) takes the absolute value of the difference between $\hat{y}$ and y:

$$\frac{1}{n}\sum_{i}^{n}|y_i - \hat{y}_i| \qquad \textbf{Equation 2}$$

The coefficient of determination, also known as the R^2 score, represents the goodness of the fit. However, relying only on the R^2 score does not necessarily guarantee a good fitting model. The

R^2 metric is normally reported with other metrics including MSE and MAE. These metrics, together with a plot that depict $y - \hat{y}$ relationship, are often used to represent the performance of a regression model [116].

Model Deployment

Another advantage of machine learning is the ability to integrate it into a production-ready platform. The convention in research when developing an optimization model, such as design of experiment (DoE) or finite element analysis (FEA), is to report the findings and possibly the effects of the different input parameters. In contrast, deploying ML in the form of a web-based software, which has been countlessly performed [24, 117-120], allows other researchers to leverage the optimization technique without needing prior knowledge in developing ML models. Further to deploying ML models in the form of web-based services, ML models have also been embedded in sensors [121, 122].

There are many considerations when translating into production ready products [123]. For computational performance consideration needs to be given to the scalability of the algorithm [124]. Moreover, as most algorithms are not autonomous, they will have to be regularly trained as the dataset expands [125]. Lastly, models tend to degrade, and thus will require regular inspection [126, 127]. The complete ML pipeline is illustratively summarised in **Figure 4**.

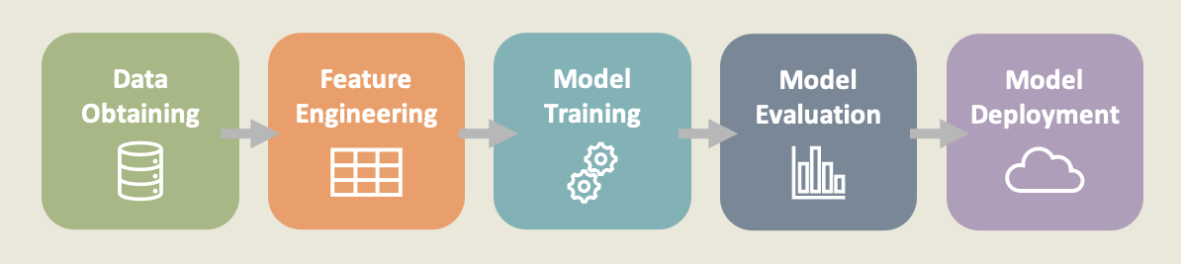

Figure 4. Schematic depicting the stages of the ML pipeline.

Machine Learning for Electrohydrodynamic Processes

The goal of ML for EHD processes is to expedite the workflow through predicting key processing parameters that otherwise would require an exhaustive trial-and-error approach. Moreover, working with relatively expensive materials such as poly-lactic-co-glycolic acid (PLGA) can result in a costly endeavour for the sake of optimization. Recently, numerous studies have demonstrated that ML can predict key processing variables; the most common ML application in EHD processing has been the prediction of fibre dimensions using ANN (**Figure *5*** & **Table 6**). The dimensions of electrospun fibres govern the quality of the product, influencing characteristics such as mechanical strength and porosity, through to more niche applications such as drug release in pharmaceutics and conductivity in biosensors [128]. Given the thickness of the fibres

typically ranging from nano to micrometer, most studies employ SEM imaging to measure the fibre diameter. However, SEM is a costly and sample-destructive characterization technique; thus the use of ML can minimise the need for SEM imaging. The importance of predicting the fibre diameter has attracted a great deal of interest, with researchers using DoE to establish a viable optimization technique. However, DoE requires specific experiments to be conducted, seldom applied to data already obtained, and struggles to handle noisy and highly correlated data. Moreover, even if a given experiment is known to fail, DoE will still need the experiment to be performed in order to build the model, at the expense of material and time. ML on the other hand can overcome the aforementioned issues, and hence less effort is spent by researchers in preparing the data. A more pertinent advantage is that ML was reported to outperform a DoE quadratic model in predicting fibre diameter (**Figure *5*(D)**) [129, 130].

Inputs used to build ANN models, i.e. the independent parameter, generally include polymer weight fraction, solvent concentration, temperature of the media, applied voltage and the collector distance; these are readily obtainable and do not require additional characterisation techniques. This strategy has been successful in predicting the fibre diameter for a broad range of polymers, including polyethylene oxide, nylon, polyacrylonitrile, polyurethane, polycaprolactone, as well as biopolymers such as gelatin, chitosan blended with polyvinyl alcohol and kefiran (**Table 6**). The neural network architectures developed do vary between the different studies, generally ranging from 1 to 3 hidden layers, suggesting that a deep and complex architecture is not necessarily needed to predict the fibre diameter, and thus the models are computationally undemanding. The models developed have been on small datasets of fewer than 50 formulations, which demonstrates that a model with good accuracy can be rapidly developed. The popularity of using ANN is further highlighted when compared with other ML algorithms. Two studies by Kalantary et al. (2019 & 2020) demonstrated ANN outperformed SVM and MLR (**Figure *5*(C)**) [131, 132]. In one study, they reported R^2 of 0.83 and 0.96 for SVM and ANN, respectively. The MAE were 60 and 0.097, respectively. In other words, ANN was able to achieve a remarkable error of +/- 0.097 nm on average in predicting the fibre diameter. When comparing ANN to MLR, the former yielded a superior accuracy, with R^2 of 0.96 and 0.56, respectively. The inability of MLR to achieve a good agreement in modelling the fibre diameter infers that the relationship between the input and target variables are nonlinear, whereas ANN can model nonlinear relationships. Further research is needed to confirm this hypothesis.

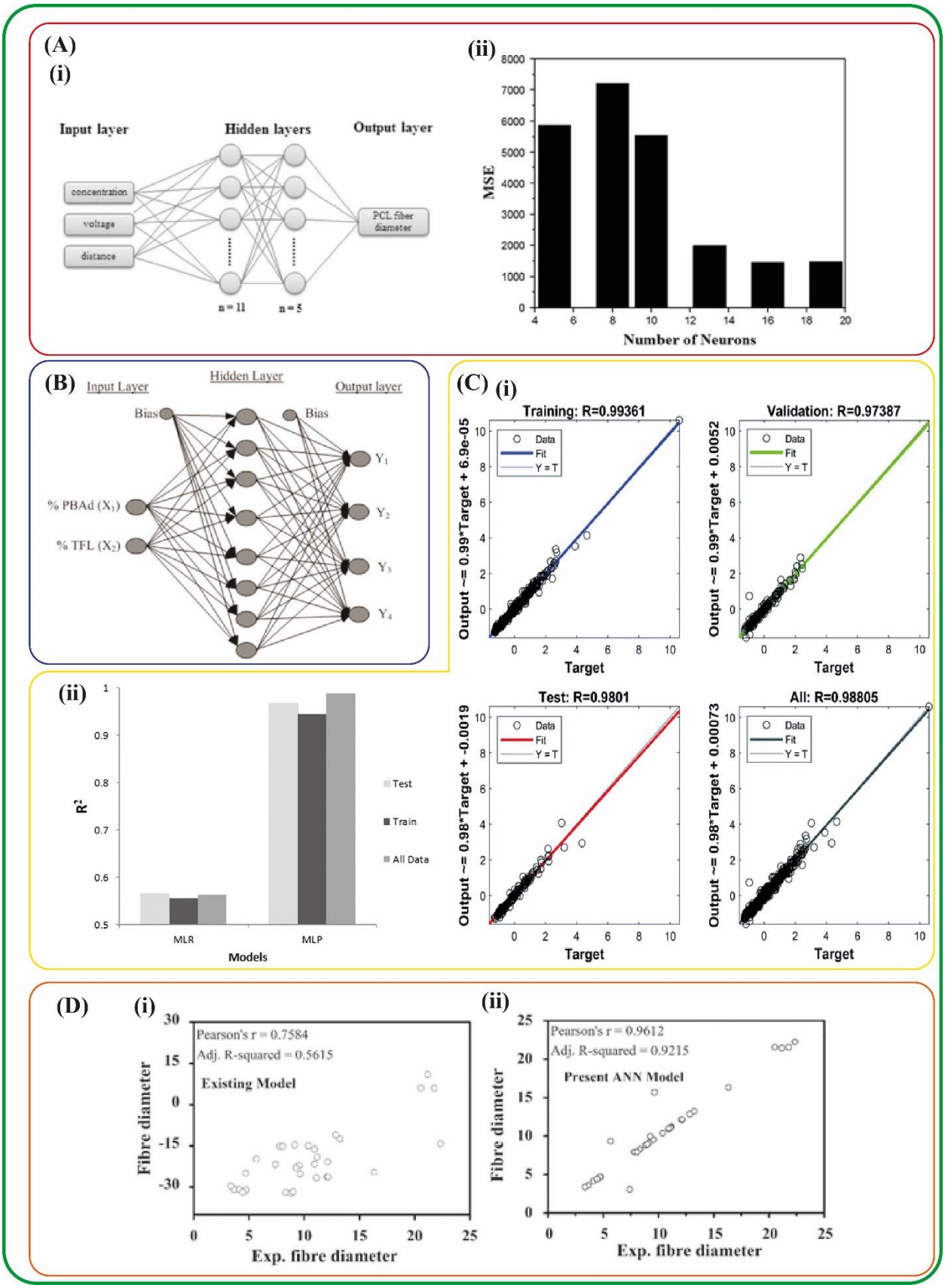
(A)
(i)
Input layer
Hidden layers
Output layer
concentration
voltage
distance
PCL fiber diameter
n = 11
n = 5
(ii)
MSE
Number of Neurons
(B)
Input Layer
Hidden Layer
Output layer
Bias
Bias
% PBAd (X1)
% TFL (X2)
Y1
Y2
Y3
Y4
(C)
(i)
Training: R=0.99361
Validation: R=0.97387
Test: R=0.9801
All: R=0.98805
Data
Fit
Y = T
Output ~= 0.99*Target + 6.9e-05
Output ~= 0.99*Target + 0.0052
Output ~= 0.98*Target + -0.0019
Output ~= 0.98*Target + 0.00073
Target
(ii)
R2
Test
Train
All Data
MLR
MLP
Models
(D)
(i)
Pearson's r = 0.7584
Adj. R-squared = 0.5615
Existing Model
Fibre diameter
Exp. fibre diameter
(ii)
Pearson's r = 0.9612
Adj. R-squared = 0.9215
Present ANN Model
Fibre diameter
Exp. fibre diameter

Figure 5 ANN is a powerful modelling technique in EHD. **(A(i))** An example of ANN used to predict the fibre diameter using three inputs. **(A(ii))** The number of hidden neurons can vary but this study found that increasing the number of hidden neurones resulted in lower prediction error [133]. **(B)** ANN can also simultaneously predict multiple outputs, which in this study was the drug release at 24, 48 and 96 hours, as well as whether burst release was observed (Y4) [134]. **(C(i))** High accuracies were obtained using ANN, **(C(ii))** particularly when compared to multi-linear regression [131]. **(D(i))** Study revealed that DoE performed poorly in predicting fibre diameter compared to **(D(ii))** ANN [129]. (X – denotes the input feature; Y – denotes the target variable; T – target)

Table 6. *ML applications of EHD*

Author	Polymer	ML Algorithm	Inputs*	Prediction	Accuracy (metric)
Nasouri [135]	PVP	ANN	Voltage, Distance, Concentration	Fibre diameter	0.981 (R^2)
Majidi et al. [136]	Nylon-6,6	ANN	Voltage, Distance, Concentration, Flow rate	Fibre diameter	0.91 (R^2)
Mirzaei et al. [137]	PEO	ANN	Polymer concentration, solvent concentration, voltage, temperature	Fibre diameter	0.83 (R^2)
Premasudha et al. [129]	Starch	ANN	polymer concentration, solution feed rate, applied voltage, nozzle to collector distance	Fibre diameter	0.92 (R^2)
Kalantary et al. [131]	PCL/gelatin	MLR, ANN, SVM	weight ratio, applied voltage, injection rate, and distance	Fibre diameter	0.96 (R^2); 0.097 (MAE)
Maurya et al. [138]	PVA	ANN	flow rate, voltage, distance, and collector rotating speed	Fibre diameter	0.79 (R^2)

Siafaka et al. [134]	PLA/PBAD	MLR, ANN	Polymer and drug concentration	Drug dissolution behaviour	0.873-0.892 (R^2)
Reisi-dehkordi et al. [139]	PAN	ANN	precursor, temperature oxidation, residence time, LTC and HTC	Fibre strength	0.972 (R^2)
Vatankhah et al. [140]	PCL/gelatin	ANN	composition, fibre diameter, alignment index and alignment direction	Elastic modulus	0.92-0.97 (R^2)
Ieracitano et al. [141]		Neural Networks	SEM images	Fibre homogeneity	
Ziaee et al. [142]	HPMCP, HPMCAS	PCA, k-means	Raman Spectroscopy	Molecular properties	-
Ball et al. [143]	PEDOT:PSS	ANN	voltage, distance, flow rate	Droplet diameter	2.51% (AAPD)
Mahmoodi et al. [144]	Zeolite-Chitosan/PVA	ANN	pH, time, MG concentration, and ZIF-8@CS/PVA-ENF(2)) dosage	Dye concentration absorption/ remediation	0.99 (R^2) 1.97 (RMSE)
Jamalabadi et al. [145]	PPy-ZnO	ANN, PCA	Concentration	Sensor response	0.81-0.98 (R^2)
Ciaburro et al. [146]	PVP-silica	ANN	Mass, Frequency	Sound Absorption Coefficient	0.94 (R) 0.057 (MAE)

*Distance refers to needle-to-collector distance

(PVP – polyvinylpolypyrrolidone; PEO – polyethylene oxide; PCL – polycaprolactone; PVA – polyvinyl alcohol; PLA – polylactide; PBAD – poly butylene adipate; PAN – polyacrylonitrile; HPMCP – Hypromellose phthalate; HPMCAS – Hypromellose acetate succinate; PEDOT:PSS - Poly(2,3-dihydrothieno-1,4-dioxin)-poly(styrenesulfonate); PPy – polypyrrole; ZnO – zinc oxide; SEM – scanning electron microscopy)

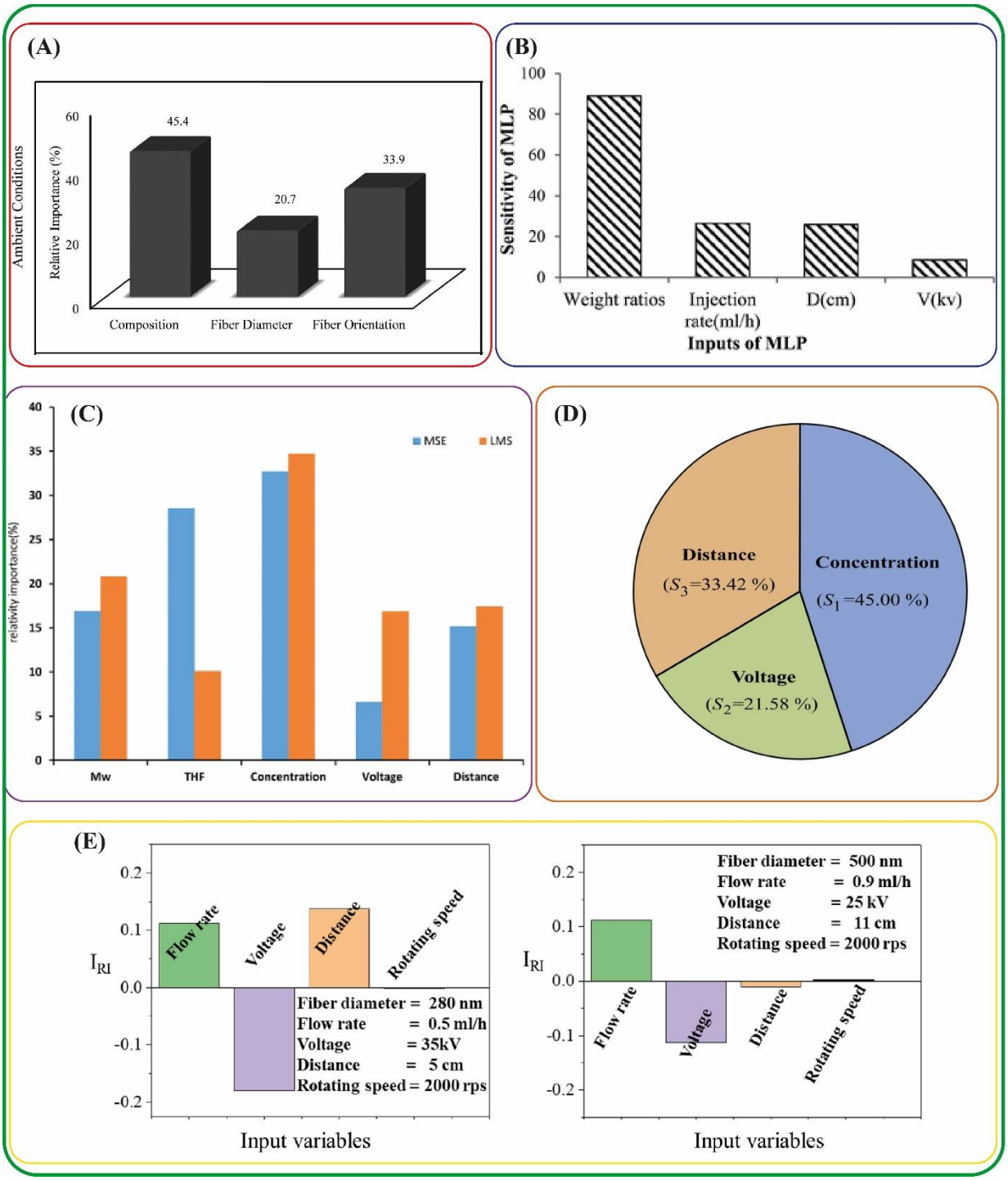

Figure 6. ANN are used to generate sensitivity analysis to determine the importance of the input variables. Generally, the starting composition has the largest influence on the final product, where analysed. The figure presents examples of sensitivity analysis for (A) the elastic modulus of Polycaprolactone/gelatin blend [140]; and the fibre diameter for (B) polycaptolactone/gelatin blends [131]; (C) polyurethane [147]; (D) poly(vinyl pyrrolidone) [135]; and poly vinyl alcohol composite [138]. (S – denotes Significance)

Some of the studies using ANN applied sensitivity analysis to determine the relationship between electrospinning parameters and fibre diameter [129], whereas others used surface response plots to determine the relationship. Sensitivity analysis is used to identify how 'sensitive' a model is to change when the input is varied [148]. For producing starch fibres, the ANN modelling elucidated an inverse relationship between fibre diameter and both spinning distance (5-8 cm) and voltage (6-10 kV), whereas a proportional relationship between starch concentration and fibre diameter was observed (10-15 w/v%) [129]. For PVP, increasing the polymer concentration (8-20 wt%) or voltage (13-23) was found to increase fibre diameter (10-20 cm), whereas increasing the spinning distance was found to decrease fibre diameter [135]. The analysis was more complicated for electrospinning nylon fibres [136]. Although the relationship between nylon concentration (16-25 w/v%) and fibre diameter was the same as the aforementioned studies, both the effect of spinning distance (6-20 cm) and voltage (16-26 kV) varied depending on the nylon concentration. For example, low and high polymer concentrations revealed an inverse relationship between spinning distance and fibre diameter, whereas at medium concentration the relationship was proportional. Maurya et al. (2020) investigated the relationship between processing parameters at specific fibre diameters of 280 and 500 nm of polyvinyl alcohol fibres blended with iron oxide nanoparticles [138]. A relative importance was derived from the ANN model, that revealed flow rate was positively correlated to fibre diameter, whereas voltage had a negative effect, and the rotating drug speed had a negligible effect. Interestingly, the study revealed the spinning distance to have a positive correlation on fibre diameter for producing fibres with 280 nm diameters, however the distance was found to have a negligible effect for fabricating fibres at the larger diameter of 500 nm. Thus, from these results it is evident that the relationship between processing parameters and fibre diameters can vary with the starting polymer. **Figure 6** presents examples of sensitivity analysis.

Aside from fibre diameter, the mechanical properties of the fibres have also been modelled using ML (**Table 6**). Although EHD can produce aligned fibres once optimised, electrospun materials typically result in non-uniform, anisotropic mechanical properties, which are difficult to model. Previous work has used finite element analysis (FEA) to model the mechanical properties of electrospun fibres, demonstrating a high resemblance to experimental data [149, 150]. However, FEA requires the properties of the investigated materials to be known before modelling, which may not be accessible. In contrast, ML does not require additional characterisation techniques to develop a model, thereby obviating the need for costly experiments to be conducted. A further minor drawback is that FEA are known to be computationally demanding. On the other hand, the go-to ML algorithm, ANN, was able to achieve R^2 values above 0.9 for the elastic modulus and fibre strength (**Table 6**). In predicting the elastic modulus, a sensitivity analysis was performed to assess the relative importance of various input variables in ANN simulations. When a high accurate model is obtained, a sensitivity analysis can be informative, aiding EHD users on which parameters to control to yield a maximum impact. In the aforementioned study, the sensitivity analysis revealed that the polymer composition was the most important factor in affecting the elastic modulus of samples. This confirms that the ANN model is learning the relationship between the input and output data, just as an expert user would but in a considerably shorter period. Interestingly, the same study used fibre diameter as an input in predicting the elastic modulus, where the fibre diameter was obtained via SEM imaging. As discussed earlier in this

section, the fibre diameter can be effectively predicted using ML, thereby potentially reducing the need for SEM or other post processing characterisation techniques in future studies for predicting the elastic modulus.

Applications of ML in EHD Processing Workflow

ML has also been applied to domain-specific applications. One area where EHD is garnering interest is in drug delivery because of its high degree of control over formulation design [151]. Although dissolution studies are necessity for the US FDA approval, the analysis for sustained release of drugs can last in the order of days to weeks. Hence, simulating this *in vitro* study can facilitate researchers in adjusting their formulations to meet a desired drug release profile, and thereby obviating the need to perform many protracted studies. Another domain-specific application of ML is predicting the removal of pollutants in wastewater treatment [144]. This is another field where EHD is attracting interest owing to its ability to process nano-sized features, and porosity design. Collectively, these studies illustrate that ML can be applied to applications where the users are more concerned with end product performance, rather than understanding the fundamentals of the processing design parameters (e.g. fibre diameter). Understandably, the complexity of domain-specific applications increases, making it challenging to be modelled with, for example, mechanistic models. In this respect, using ML may prove to be a simpler modelling approach. For example, in the case of drug dissolution, including information about drug solubility, dissolution pH and dissolution volume – in addition to EHD processing parameters – will result in a complex modelling relationship, which fortunately ML can model.

The aforementioned studies demonstrate the utility of ANN for achieving good predictive performance on low-sample datasets. It is worth acknowledging that the transferability of the models is yet to be tested, whether it is changing the EHD process parameters (e.g. applied voltage, needle gauge, collecting distance, etc.), or using the same polymer but with a different molecular weight. Moreover, the models cannot be transferred to novel polymers, and so will become time consuming when a large number of polymers need to be modelled. Alternatively, polymer informatics can be exploited, wherein the inputs of the polymer pertain to their chemical structure [152]. Thus, once the ML model learns the relationship between the chemical structure to e.g. fibre diameter, it can be generalised to new polymers not found in the training set. Nevertheless, the aforementioned examples demonstrate the potency of ANN for small-scale production.

Machine Learning for Image Classification

What is also remarkable about ML is that a pipeline can be developed for image analysis. Undeniably, imaging is an important aspect of quality control, ensuring a defect-free product has been produced. Despite their importance, the process of scanning and analysing images can be laborious, and subject to human bias in interpreting the results. Recent work has investigated the possibility of employing ML for image classification to overcome the aforementioned issues, where it was reported that ML is capable of emulating experts in detecting defects in electrospun

fibres [141]. When combined with the fact that the predictions can be made in a matter of seconds, ML does indeed offer a powerful strategy to classifying images manually [141, 153].

The 'gold standard' in ML algorithms for images is CNN, which is a network-based ML, but compared with neural networks with similar sized layers, CNNs have fewer connections and parameters, and thus are easier to train [154]. Moreover, CNNs are able to capture the non-linearity in datasets; non-linearity is commonly found in images, such as photographs and electron micrographs, because of a number of elements [155-160]. Two studies have demonstrated the feasibility of utilising CNN for EHD process monitoring. One study investigated CNN for classifying images of the "Taylor cone jet", which is the optimal jetting behaviour of EHD, produced during EHD processing, obtained from a digital microscope [161]. Given that environmental parameters such as humidity and temperature can have distinct effects on the Taylor cone jet mode, the processing parameters will need to be accommodated accordingly. Hence, an efficient monitoring system is required. For that work, 5000 images were taken of EHD processing of PCL solutions, in which between 500-4000 images were used to train the CNN model, 500 images were used for validation and a further 500 images were used for testing. The images were classified into eight different Taylor cone modes. It was revealed that the test accuracy increased as the training size increased from 88.9% for training on 500 images to 94.7% for training on 4000 images. In a separate study, ML was used to classify images obtained from a polarized light microscope [162]. This imaging modality is also suitable for real-time measurements. For this particular approach, pairing polarized images with CNN was found to predict accurately the morphology of electrospun PLLA and PCL, with a test accuracy of 96.15% in classifying whether the fibres were smooth, microporous or beaded [162].

Despite its high performing results, a key drawback to CNN is that the algorithm is data hungry, requiring large numbers of samples to achieve high accuracies, which may not be feasible to users who are unable to generate large datasets due to time or cost constraints. Fortunately, an alternative approach was recently demonstrated by Leracitano et al. (2020) who combined an Autoencoder (AE) with ANN, to identify defects in electrospun fibres [141]. Feature selection and dimensionality reduction are widely employed to improve the performance of MLTs [163, 164]. Although one feature of ML is its ability to compute high-dimensionality data, not every additional feature is useful (i.e. noisy). Thus, dimensionality reduction algorithms are employed to minimise the number of dimensions, with both PCA and AE found to be effective at reducing the noise in high-dimensional data [165]. PCA is the more commonly-used technique for identifying the most relevant features to use from an image, thanks to its simplicity. There is, of course, the added benefit that reducing the number of inputs can also reduce the computational demands of the process, resulting in a faster prediction time. Whilst PCA has been demonstrated to be effective for feature selection, it is limited to linear features. AE on the other hand can handle both linear and non-linear datasets. An AE takes in all the features of an image as a node, and discards redundant features, providing an output of nodes with the most relevant features [166, 167]. Leracitano et al. (2020) employed an AE as a feature extraction to extract the most relevant features from SEM micrographs of electrospun fibres. Finding the features that are distinct between different classes of images is indeed a near-impossible task for researchers to perform manually, given the considerably large number of pixels an image can generate, and that

each pixel can possess a wide range of colour shades. However, this is an easy task for a well-trained AE and thus employing an Autoencoder can relieve a user of this daunting task. For their study, Leracitano et al. (2020) developed a model using 160 images and an AE to differentiate between the features obtained from images containing an undesirable bead to that of micrographs containing homogenous fibres. Following the feature extraction, ANN was used to classify the data. This two-step ML approach resulted in a classification accuracy of 92.5%, which was higher than the 80% accuracy obtained by CNN using the same sample size. The ability of ML to accommodate different data formats broadens their applicability. **Table *7*** provides a summary of the advantages of ML algorithms, as well as their drawbacks.

Table 7. A summary of the advantages and drawbacks of ML algorithms.

Algorithm	Advantages	Drawbacks
MLR	• Transparent	• Not suitable for non-linear data
LR	• Transparent	• Not suitable for non-linear data
RF	• Insensitive to outliers	• Computationally expensive
GBDT	• Insensitive to outliers	• Computationally expensive
MLP	• Can handle non-linear data	• Requires pre-processing of data
CNN	• Can handle images	• Requires a large dataset
RNN	• Learns sequential events, such as dynamic systems	• Complex building stage
SVM	• Can handle both linear and non-linear data	• Computationally expensive • Sensitive to outliers
kNN	• Simple to use	• Accuracy decreases with high-dimensional data
NB	• Minimal parameter tuning	• Accuracy decreases if the input features are dependent
k-means	• Can cluster on large dataset	• Does not perform well in global searching
GMM	• Speed • Training stability	• Complex building stage
PCA	• Can de-noise the dataset	• Not suitable for non-linear data
Generative Models	• Generates new data	• Model training can be unstable

Outlook and Concluding Remarks

The aforementioned examples highlight the potential of ML for image classification to facilitate EHD processing, and to expedite the translation of impactful research into clinical applications. The ability to distinguish between the Taylor cone jet modes can help towards building a reliable

automated monitoring system, particularly for complex systems such as multi-nozzle EHD. The possibility to build ML models on relatively small datasets is indeed appealing. This has been a subject of interest to the ML community. As a response, 'few shot' and 'one shot' learning models have been developed, and they have had profound benefits across a number of disciplines [168, 169]. As the name suggests, such models require either a few or one, respectively, samples to develop a model. Hence, researchers in EHD have several ML options available, depending on their constraints. Needless to say, the use of ML image classification remains nascent, and there is opportunity to explore other imaging modalities, such as x-ray microtomography, transmission electron microscopy, and hyperspectral images [170-173].

In the past decade, with the increasing knowledge in the area of nanotechnology, there is a widespread demand in the use of simple, versatile and cost-effective processing techniques for the fabrication of nanostructures. EHD process has recently drawn an enormous attention due to its capability to produce products in nano to micron- size range from various types of raw materials. The successful commercialisation and FDA approval of a number of nanofiber products produced by electrospinning, and the great potential in the development of novel polymeric nano/microparticles from the related electrospraying process, should drive extensive efforts in the advancement into the field to improve the EHD process monitoring and control.

Despite numerous studies developing theoretical models and simulations for better understanding of the mechanisms involved in the process of EHD, large-scale production of micro/nano features from this technique is still hindered by the complex behaviour of the electrified jets and lack of predictive models that encompass a plethora of process parameters. Whilst EHD process exhibits high flexibility towards processing of a variety of materials with multiple functionalities through co-axial and multi-axial technologies, there is still a strong need to address issues concerning large-volume processing as well as accuracy and reproducibility. In addition, translation of the EHD process to industry requires the know-how and multidisciplinary knowledge by the operators and users of the equipment. With the aid of the state-of-the-art predictive models such as ML, the key EHD process parameters as well as the overall EHD workflow can be regulated to achieve a more sustainable manufacturing process in the near future. ML can facilitate process monitoring and quality control through in-line systems and automation. The EHD process can become more intelligent and efficient through integration with ML, reducing the production time and enhancing the product quality. As discussed in this review, so far, there has only been a few attempts to develop ML algorithms in the EHD process workflow. Notwithstanding, continuous research efforts are still required to develop more accurate ML models to allow improvements in the current EHD technologies. It is evident that the industry is undergoing a paradigm shift with engineering principals and product-process design guiding manufacturing. Further developments in ML for the EHD process can eventually transform this technology and its products toward commercialisation.

Ultimately, EHD processes have the potential to address gaps in healthcare research. Further work is needed to refine the EHD processes, particularly to advance EHD processes that can develop 3D products. Here, ML will be required to help expedite the formulation development stage of advanced EHD processes, and to minimise the empirical trial-and-error methodology

that will not yield sustainable research in the future. The application of ML for EHD processes is beginning to garner interest, however, a cross-disciplinary workforce encompassing ML practitioners, informaticians and EHD researchers, will be needed to harness the prospect of ML for EHD processes.

References

[1] A. Reiser, M. Lindén, P. Rohner, A. Marchand, H. Galinski, A.S. Sologubenko, J.M. Wheeler, R. Zenobi, D. Poulikakos, R. Spolenak, Multi-metal electrohydrodynamic redox 3D printing at the submicron scale, Nature Communications 10(1) (2019) 1853.
[2] M.S. Onses, E. Sutanto, P.M. Ferreira, A.G. Alleyne, J.A. Rogers, Mechanisms, Capabilities, and Applications of High-Resolution Electrohydrodynamic Jet Printing, Small 11(34) (2015) 4237-4266.
[3] L.A. Mercante, V.P. Scagion, F.L. Migliorini, L.H.C. Mattoso, D.S. Correa, Electrospinning-based (bio)sensors for food and agricultural applications: A review, TrAC Trends in Analytical Chemistry 91 (2017) 91-103.
[4] B. Azimi, M. Milazzo, A. Lazzeri, S. Berrettini, M.J. Uddin, Z. Qin, M.J. Buehler, S. Danti, Electrospinning Piezoelectric Fibers for Biocompatible Devices, Advanced Healthcare Materials 9(1) (2020) 1901287.
[5] K.D. Patel, H.-W. Kim, J.C. Knowles, A. Poma, Molecularly Imprinted Polymers and Electrospinning: Manufacturing Convergence for Next-Level Applications, Advanced Functional Materials 30(32) (2020) 2001955.
[6] F. Croisier, G. Atanasova, Y. Poumay, C. Jérôme, Polysaccharide-Coated PCL Nanofibers for Wound Dressing Applications, Advanced Healthcare Materials 3(12) (2014) 2032-2039.
[7] M.E. Alkahtani, A.H. Aodah, O.A. Abu Asab, A.W. Basit, M. Orlu, E.A. Tawfik, Fabrication and Characterization of Fast-Dissolving Films Containing Escitalopram/Quetiapine for the Treatment of Major Depressive Disorder, Pharmaceutics 13(6) (2021) 891.
[8] J. Xie, J. Jiang, P. Davoodi, M.P. Srinivasan, C.-H. Wang, Electrohydrodynamic atomization: A two-decade effort to produce and process micro-/nanoparticulate materials, Chemical Engineering Science 125 (2015) 32-57.
[9] W. Balachandran, P. Miao, P. Xiao, Electrospray of fine droplets of ceramic suspensions for thin-film preparation, Journal of Electrostatics 50(4) (2001) 249-263.
[10] J. Voorneveld, A. Oosthuysen, T. Franz, P. Zilla, D. Bezuidenhout, Dual electrospinning with sacrificial fibers for engineered porosity and enhancement of tissue ingrowth, Journal of Biomedical Materials Research Part B: Applied Biomaterials 105(6) (2017) 1559-1572.
[11] N. Radacsi, F.D. Campos, C.R.I. Chisholm, K.P. Giapis, Spontaneous formation of nanoparticles on electrospun nanofibres, Nature Communications 9(1) (2018) 4740.
[12] K.-H. Lee, S.-S. Lee, D.B. Ahn, J. Lee, D. Byun, S.-Y. Lee, Ultrahigh areal number density solid-state on-chip microsupercapacitors via electrohydrodynamic jet printing, Science Advances 6(10) (2020) eaaz1692.
[13] S. Moon, M.S. Jones, E. Seo, J. Lee, L. Lahann, J.H. Jordahl, K.J. Lee, J. Lahann, 3D jet writing of mechanically actuated tandem scaffolds, Science Advances 7(16) (2021) eabf5289.

[14] X. Xu, A. Seijo-Rabina, A. Awad, C. Rial, S. Gaisford, A.W. Basit, A. Goyanes, Smartphone-enabled 3D printing of medicines, International Journal of Pharmaceutics 609 (2021) 121199.
[15] Y. Kuwahata, H. Takehara, T. Ichiki, Comprehensive study on electrospray deposition in the single Taylor cone–jet mode by changing the spatial electric potential using a ring-shaped ternary electrode, AIP Advances 10(4) (2020) 045107.
[16] L. Jiang, L. Yu, P. Premaratne, Z. Zhang, H. Qin, CFD-based numerical modeling to predict the dimensions of printed droplets in electrohydrodynamic inkjet printing, Journal of Manufacturing Processes 66 (2021) 125-132.
[17] Y. Su, H. Jiang, Z. Liu, An experimental investigation on heat transfer performance of electrostatic spraying used in machining, The International Journal of Advanced Manufacturing Technology 112(5) (2021) 1285-1294.
[18] K. Mohammadi, M.R. Movahhedy, S. Khodaygan, Colloidal particle reaction and aggregation control in the Electrohydrodynamic 3D printing technology, International Journal of Mechanical Sciences 195 (2021) 106222.
[19] S. Ekins, A.C. Puhl, K.M. Zorn, T.R. Lane, D.P. Russo, J.J. Klein, A.J. Hickey, A.M. Clark, Exploiting machine learning for end-to-end drug discovery and development, Nature Materials 18(5) (2019) 435-441.
[20] M. Elbadawi, L.E. McCoubrey, F.K.H. Gavins, J.J. Ong, A. Goyanes, S. Gaisford, A.W. Basit, Disrupting 3D printing of medicines with machine learning, Trends in Pharmacological Sciences 42(9) (2021) 745-757.
[21] A. Awad, S.J. Trenfield, T.D. Pollard, J.J. Ong, M. Elbadawi, L.E. McCoubrey, A. Goyanes, S. Gaisford, A.W. Basit, Connected healthcare: Improving patient care using digital health technologies, Advanced Drug Delivery Reviews 178 (2021) 113958.
[22] B. Muñiz Castro, M. Elbadawi, J.J. Ong, T. Pollard, Z. Song, S. Gaisford, G. Pérez, A.W. Basit, P. Cabalar, A. Goyanes, Machine learning predicts 3D printing performance of over 900 drug delivery systems, Journal of Controlled Release 337 (2021) 530-545.
[23] L.E. McCoubrey, S. Gaisford, M. Orlu, A.W. Basit, Predicting drug-microbiome interactions with machine learning, Biotechnology Advances (2021) 107797.
[24] M. Elbadawi, B. Muñiz Castro, F.K.H. Gavins, J.J. Ong, S. Gaisford, G. Pérez, A.W. Basit, P. Cabalar, A. Goyanes, M3DISEEN: A novel machine learning approach for predicting the 3D printability of medicines, International Journal of Pharmaceutics 590 (2020) 119837.
[25] A.W. Senior, R. Evans, J. Jumper, J. Kirkpatrick, L. Sifre, T. Green, C. Qin, A. Žídek, A.W.R. Nelson, A. Bridgland, H. Penedones, S. Petersen, K. Simonyan, S. Crossan, P. Kohli, D.T. Jones, D. Silver, K. Kavukcuoglu, D. Hassabis, Improved protein structure prediction using potentials from deep learning, Nature 577(7792) (2020) 706-710.
[26] V. Rotemberg, N. Kurtansky, B. Betz-Stablein, L. Caffery, E. Chousakos, N. Codella, M. Combalia, S. Dusza, P. Guitera, D. Gutman, A. Halpern, B. Helba, H. Kittler, K. Kose, S. Langer, K. Lioprys, J. Malvehy, S. Musthaq, J. Nanda, O. Reiter, G. Shih, A. Stratigos, P. Tschandl, J. Weber, H.P. Soyer, A patient-centric dataset of images and metadata for identifying melanomas using clinical context, Scientific Data 8(1) (2021) 34.
[27] Y. Gurovich, Y. Hanani, O. Bar, G. Nadav, N. Fleischer, D. Gelbman, L. Basel-Salmon, P.M. Krawitz, S.B. Kamphausen, M. Zenker, L.M. Bird, K.W. Gripp, Identifying facial phenotypes of genetic disorders using deep learning, Nature Medicine 25(1) (2019) 60-64.

[28] M. Elbadawi, S. Gaisford, A.W. Basit, Advanced machine-learning techniques in drug discovery, Drug Discovery Today 26(3) (2021) 769-777.
[29] E. Schwager, K. Jansson, A. Rahman, S. Schiffer, Y. Chang, G. Boverman, B. Gross, M. Xu-Wilson, P. Boehme, H. Truebel, J.J. Frassica, Utilizing machine learning to improve clinical trial design for acute respiratory distress syndrome, npj Digital Medicine 4(1) (2021) 133.
[30] X. Zhang, H. Wang, Y. Tian, L. Peyrodie, X. Wang, Model-free based neural network control with time-delay estimation for lower extremity exoskeleton, Neurocomputing 272 (2018) 178-188.
[31] J. Yoon, J. Han, J.I. Park, J.S. Hwang, J.M. Han, J. Sohn, K.H. Park, D.D.-J. Hwang, Optical coherence tomography-based deep-learning model for detecting central serous chorioretinopathy, Scientific Reports 10(1) (2020) 18852.
[32] M.R. Ali, T. Myers, E. Wagner, H. Ratnu, E.R. Dorsey, E. Hoque, Facial expressions can detect Parkinson's disease: preliminary evidence from videos collected online, npj Digital Medicine 4(1) (2021) 129.
[33] W. Yu, T. Liu, R. Valdez, M. Gwinn, M.J. Khoury, Application of support vector machine modeling for prediction of common diseases: the case of diabetes and pre-diabetes, BMC Medical Informatics and Decision Making 10(1) (2010) 16.
[34] E. Choi, A. Schuetz, W.F. Stewart, J. Sun, Using recurrent neural network models for early detection of heart failure onset, Journal of the American Medical Informatics Association 24(2) (2016) 361-370.
[35] Z. Ji, Y. Xia, Q. Sun, Q. Chen, D. Feng, Adaptive scale fuzzy local Gaussian mixture model for brain MR image segmentation, Neurocomputing 134 (2014) 60-69.
[36] T.M. Mitchell, Machine Learning, 1 ed., McGraw-Hill, Inc., USA, 1997.
[37] I.V. Tetko, P. Karpov, R. Van Deursen, G. Godin, State-of-the-art augmented NLP transformer models for direct and single-step retrosynthesis, Nature Communications 11(1) (2020) 5575.
[38] R. Ramprasad, R. Batra, G. Pilania, A. Mannodi-Kanakkithodi, C. Kim, Machine learning in materials informatics: recent applications and prospects, npj Computational Materials 3(1) (2017) 1-13.
[39] V. Tshitoyan, J. Dagdelen, L. Weston, A. Dunn, Z. Rong, O. Kononova, K.A. Persson, G. Ceder, A. Jain, Unsupervised word embeddings capture latent knowledge from materials science literature, Nature 571(7763) (2019) 95-98.
[40] M. Elbadawi, S. Gaisford, A.W. Basit, Advanced machine-learning techniques in drug discovery, Drug Discovery Today (2020).
[41] H. Narayanan, F. Dingfelder, A. Butté, N. Lorenzen, M. Sokolov, P. Arosio, Machine Learning for Biologics: Opportunities for Protein Engineering, Developability, and Formulation, Trends in Pharmacological Sciences 42(3) (2021) 151-165.
[42] J. Vamathevan, D. Clark, P. Czodrowski, I. Dunham, E. Ferran, G. Lee, B. Li, A. Madabhushi, P. Shah, M. Spitzer, S. Zhao, Applications of machine learning in drug discovery and development, Nature Reviews Drug Discovery 18(6) (2019) 463-477.
[43] L.E. McCoubrey, M. Elbadawi, M. Orlu, S. Gaisford, A.W. Basit, Machine Learning Uncovers Adverse Drug Effects on Intestinal Bacteria, Pharmaceutics 13(7) (2021) 1026.
[44] J. Devlin, M.-W. Chang, K. Lee, K. Toutanova, BERT: Pre-training of Deep Bidirectional Transformers for Language Understanding, arXiv:1810.04805 [cs] (2019).

[45] J. Janai, F. Güney, A. Behl, A. Geiger, Computer Vision for Autonomous Vehicles: Problems, Datasets and State of the Art, Foundations and Trends® in Computer Graphics and Vision 12(1–3) (2020) 1-308.
[46] Y. Sun, X. Wang, X. Tang, Deep Learning Face Representation by Joint Identification-Verification, arXiv:1406.4773 [cs] (2014).
[47] K.T. Butler, D.W. Davies, H. Cartwright, O. Isayev, A. Walsh, Machine learning for molecular and materials science, Nature 559(7715) (2018) 547-555.
[48] M.I. Jordan, T.M. Mitchell, Machine learning: Trends, perspectives, and prospects, Science 349(6245) (2015) 255-260.
[49] D.C. Elton, Z. Boukouvalas, M.D. Fuge, P.W. Chung, Deep learning for molecular design - a review of the state of the art, Molecular Systems Design & Engineering 4(4) (2019) 828-849.
[50] B.J. Erickson, P. Korfiatis, Z. Akkus, T.L. Kline, Machine Learning for Medical Imaging, Radiographics 37(2) (2017) 505-515.
[51] L. Xie, L. Xu, R. Kong, S. Chang, X. Xu, Improvement of Prediction Performance With Conjoint Molecular Fingerprint in Deep Learning, Frontiers in Pharmacology 11 (2020).
[52] N. Cristianini, J. Shawe-Taylor, D.o.C.S.R.H.J. Shawe-Taylor, An Introduction to Support Vector Machines and Other Kernel-based Learning Methods, Cambridge University Press2000.
[53] L. Rokach, O.Z. Maimon, ProQuest, L. Rokach, Data mining with decision trees : theory and applications, World Scientific, Singapore, 2008.
[54] L. Breiman, Random forests, Mach Learn 45(1) (2001) 5-32.
[55] J.H. Friedman, Greedy function approximation: A gradient boosting machine., The Annals of Statistics 29(5) (2001) 1189-1232.
[56] K. Hornik, M. Stinchcombe, H. White, Multilayer feedforward networks are universal approximators, Neural Networks 2(5) (1989) 359-366.
[57] C.C. Aggarwal, SpringerLink, Neural Networks and Deep Learning : A Textbook, Springer International Publishing : Imprint: Springer, Cham, 2018.
[58] K. He, X. Zhang, S. Ren, J. Sun, Deep Residual Learning for Image Recognition, arXiv:1512.03385 [cs] (2015).
[59] K. Simonyan, A. Zisserman, Very Deep Convolutional Networks for Large-Scale Image Recognition, arXiv pre-print server (2015).
[60] G.E. Hinton, T.J. Sejnowski, Unsupervised learning foundations of neural computation, 1999.
[61] A. Kumar, Analysis of unsupervised dimensionality reduction techniques, Computer Science and Information Systems 6(2) (2009) 217-227.
[62] I.J. Goodfellow, J. Pouget-Abadie, M. Mirza, B. Xu, D. Warde-Farley, S. Ozair, A. Courville, Y. Bengio, Generative Adversarial Networks, arXiv:1406.2661 [cs, stat] (2014).
[63] D.P. Kingma, M. Welling, An Introduction to Variational Autoencoders, Foundations and Trends® in Machine Learning 12(4) (2019) 307-392.
[64] J. Ghasemi, S. Saaidpour, Quantitative structure–property relationship study of n-octanol–water partition coefficients of some of diverse drugs using multiple linear regression, Analytica Chimica Acta 604(2) (2007) 99-106.
[65] J.M. Luco, F.H. Ferretti, QSAR based on multiple linear regression and PLS methods for the anti-HIV activity of a large group of HEPT derivatives, Journal of Chemical Information and Computer Sciences 37(2) (1997) 392-401.

[66] C.R. Boyd, M.A. Tolson, W.S. Copes, Evaluating Trauma Care: The TRISS Method, Journal of Trauma and Acute Care Surgery 27(4) (1987) 370–378.
[67] G.X. Gu, C.T. Chen, M.J. Buehler, De novo composite design based on machine learning algorithm, Extreme Mech Lett 18 (2018) 19-28.
[68] A.S. Krishnapriyan, M. Haranczyk, D. Morozov, Topological Descriptors Help Predict Guest Adsorption in Nanoporous Materials, J Phys Chem C 124(17) (2020) 9360-9368.
[69] A.O. Oliynyk, E. Antono, T.D. Sparks, L. Ghadbeigi, M.W. Gaultois, B. Meredig, A. Mar, High-Throughput Machine-Learning-Driven Synthesis of Full-Heusler Compounds, Chemistry of Materials 28(20) (2016) 7324-7331.
[70] R. Gaillac, S. Chibani, F.X. Coudert, Speeding Up Discovery of Auxetic Zeolite Frameworks by Machine Learning, Chemistry of Materials 32(6) (2020) 2653-2663.
[71] J.D. Evans, F.X. Couder, Predicting the Mechanical Properties of Zeolite Frameworks by Machine Learning, Chemistry of Materials 29(18) (2017) 7833-7839.
[72] J. Devillers, Neural networks in QSAR and drug design, Acad. Press, London, 1996.
[73] S. Malinov, W. Sha, J.J. McKeown, Modelling the correlation between processing parameters and properties in titanium alloys using artificial neural network, Comp Mater Sci 21(3) (2001) 375-394.
[74] W. Sha, K.L. Edwards, The use of artificial neural networks in materials science based research, Materials & Design 28(6) (2007) 1747-1752.
[75] D. Duvenaud, D. Maclaurin, J. Aguilera-Iparraguirre, R. Gómez-Bombarelli, T. Hirzel, A. Aspuru-Guzik, R.P. Adams, Convolutional Networks on Graphs for Learning Molecular Fingerprints, arXiv:1509.09292 [cs, stat] (2015).
[76] S. Kearnes, K. McCloskey, M. Berndl, V. Pande, P. Riley, Molecular graph convolutions: moving beyond fingerprints, Journal of computer-aided molecular design 30(8) (2016) 595-608.
[77] N. Chen, ProQuest, Support vector machine in chemistry, World Scientific, Singapore ; Hackensack, N.J, 2004.
[78] E. Byvatov, U. Fechner, J. Sadowski, G. Schneider, Comparison of support vector machine and artificial neural network systems for drug/nondrug classification, Journal of Chemical Information and Computer Sciences 43(6) (2003) 1882-1889.
[79] S.J. Huang, N.G. Cai, P.P. Pacheco, S. Narandes, Y. Wang, W.N. Xu, Applications of Support Vector Machine (SVM) Learning in Cancer Genomics, Cancer Genom Proteom 15(1) (2018) 41-51.
[80] W.F. Zheng, A. Tropsha, Novel variable selection quantitative structure-property relationship approach based on the k-nearest-neighbor principle, Journal of Chemical Information and Computer Sciences 40(1) (2000) 185-194.
[81] C. Hu, G. Jain, P.Q. Zhang, C. Schmidt, P. Gomadam, T. Gorka, Data-driven method based on particle swarm optimization and k-nearest neighbor regression for estimating capacity of lithium-ion battery, Appl Energ 129 (2014) 49-55.
[82] O. Addin, S.M. Sapuan, E. Mahdi, A. Othman, A Naive-Bayes classifier for damage detection in engineering materials, Materials & Design 28(8) (2007) 2379-2386.
[83] J. Lu, L. Chen, J. Yin, T. Huang, Y. Bi, X.Y. Kong, M.Y. Zheng, Y.D. Cai, Identification of new candidate drugs for lung cancer using chemical-chemical interactions, chemical-protein interactions and a K-means clustering algorithm, J Biomol Struct Dyn 34(4) (2016) 906-917.

[84] H. Chan, M. Cherukara, T.D. Loeffler, B. Narayanan, S.K.R.S. Sankaranarayanan, Machine learning enabled autonomous microstructural characterization in 3D samples, Npj Computational Materials 6(1) (2020).
[85] C.P. Lim, S.S. Quek, K.K. Peh, Application of the Gaussian mixture model to drug dissolution profiles prediction, Neural Comput Appl 14(4) (2005) 345-352.
[86] K. Rajan, C. Suh, P.F. Mendez, Principal component analysis and dimensional analysis as materials informatics tools to reduce dimensionality in materials science and engineering, Statistical Analysis and Data Mining: The ASA Data Science Journal 1(6) (2009) 361-371.
[87] A. Belianinov, Q. He, M. Kravchenko, S. Jesse, A. Borisevich, S.V. Kalinin, Identification of phases, symmetries and defects through local crystallography, Nature Communications 6 (2015).
[88] A. Kadurin, S. Nikolenko, K. Khrabrov, A. Aliper, A. Zhavoronkov, druGAN: An Advanced Generative Adversarial Autoencoder Model for de Novo Generation of New Molecules with Desired Molecular Properties in Silico, Molecular Pharmaceutics 14(9) (2017) 3098-3104.
[89] J. Lim, S. Ryu, J.W. Kim, W.Y. Kim, Molecular generative model based on conditional variational autoencoder for de novo molecular design, Journal of Cheminformatics 10(1) (2018) 31.
[90] Z. Yang, X. Li, L.C. Brinson, A.N. Choudhary, W. Chen, A. Agrawal, Microstructural Materials Design via Deep Adversarial Learning Methodology, Journal of Mechanical Design 140(11) (2018) 111416.
[91] A. Zheng, A. Casari, Feature engineering for machine learning: principles and techniques for data scientists, First edition ed., O'Reilly, Beijing : Boston, 2018.
[92] N.M. O'Boyle, R.A. Sayle, Comparing structural fingerprints using a literature-based similarity benchmark, Journal of Cheminformatics 8 (2016).
[93] A. Ziletti, D. Kumar, M. Scheffler, L.M. Ghiringhelli, Insightful classification of crystal structures using deep learning, Nature Communications 9(1) (2018) 2775.
[94] I.T. Jolliffe, Principal Component Analysis, Springer New York, s.l., 2002.
[95] Y. Goldberg, Neural network methods in natural language processing, Morgan & Claypool, San Rafael, California, 2017.
[96] X. Li, D. Fourches, SMILES Pair Encoding: A Data-Driven Substructure Tokenization Algorithm for Deep Learning, (2020).
[97] T.-S. Lin, C.W. Coley, H. Mochigase, H.K. Beech, W. Wang, Z. Wang, E. Woods, S.L. Craig, J.A. Johnson, J.A. Kalow, K.F. Jensen, B.D. Olsen, BigSMILES: A Structurally-Based Line Notation for Describing Macromolecules, ACS Central Science 5(9) (2019) 1523-1531.
[98] D. Weininger, Smiles, a Chemical Language and Information-System .1. Introduction to Methodology and Encoding Rules, Journal of Chemical Information and Computer Sciences 28(1) (1988) 31-36.
[99] T. Le, R. Winter, F. Noe, D.A. Clevert, Neuraldecipher - reverse-engineering extended-connectivity fingerprints (ECFPs) to their molecular structures, Chemical Science 11(38) (2020) 10378-10389.
[100] S. Jaeger, S. Fulle, S. Turk, Mol2vec: Unsupervised Machine Learning Approach with Chemical Intuition, Journal of Chemical Information and Modeling 58(1) (2018) 27-35.

[101] J.L. Durant, B.A. Leland, D.R. Henry, J.G. Nourse, Reoptimization of MDL keys for use in drug discovery, Journal of Chemical Information and Computer Sciences 42(6) (2002) 1273-1280.
[102] L. Ward, A. Agrawal, A. Choudhary, C. Wolverton, A general-purpose machine learning framework for predicting properties of inorganic materials, Npj Computational Materials 2 (2016).
[103] D. Jha, L. Ward, A. Paul, W.K. Liao, A. Choudhary, C. Wolverton, A. Agrawal, ElemNet: Deep Learning the Chemistry of Materials From Only Elemental Composition, Scientific Reports 8 (2018).
[104] H. Ramchoun, Y. Ghanou, M. Ettaouil, M.A.J. Idrissi, Multilayer Perceptron: Architecture Optimization and Training, International Journal of Interactive Multimedia and Artificial Intelligence 4(Special Issue on Artificial Intelligence Underpinning) (2016).
[105] T. Agrawal, Hyperparameter optimization in machine learning: make your machine learning and deep learning models more efficient, 2021.
[106] J. Bergstra, R. Bardenet, Y. Bengio, B. Kégl, Algorithms for Hyper-Parameter Optimization, 25th Annual Conference on Neural Information Processing Systems (NIPS 2011), Neural Information Processing Systems Foundation, 2011.
[107] J. Bergstra, Y. Bengio, Random Search for Hyper-Parameter Optimization, J Mach Learn Res 13 (2012) 281-305.
[108] F. Pedregosa, G. Varoquaux, A. Gramfort, V. Michel, B. Thirion, O. Grisel, M. Blondel, P. Prettenhofer, R. Weiss, V. Dubourg, Scikit-learn: Machine learning in Python, the Journal of machine Learning research 12 (2011) 2825-2830.
[109] S. Arlot, A. Celisse, A survey of cross-validation procedures for model selection, Statistics Surveys 4(none) (2010) 40-79.
[110] R. Garreta, G. Moncecchi, ProQuest, Learning scikit-learn : machine learning in Python, Packt Publishing, Birmingham, 2013.
[111] B. Efron, The jackknife, the bootstrap, and other resampling plans, Society for Industrial and Applied Mathematics, Philadelphia, Pa, 1982.
[112] C. Sammut, G.I. Webb, Leave-One-Out Cross-Validation, in: C. Sammut, G.I. Webb (Eds.), Encyclopedia of Machine Learning, Springer US, Boston, MA, 2010, pp. 600-601.
[113] V. Bewick, L. Cheek, J. Ball, Statistics review 13: Receiver operating characteristic curves, Critical Care 8(6) (2004) 508.
[114] D.M. Powers, Evaluation: from precision, recall and F-measure to ROC, informedness, markedness and correlation, arXiv preprint arXiv:2010.16061 (2020).
[115] D. Carlin, P. O'Kane, S. Sezer, A cost analysis of machine learning using dynamic runtime opcodes for malware detection, Computers & Security 85 (2019) 138-155.
[116] S. Raschka, Model Evaluation, Model Selection, and Algorithm Selection in Machine Learning, arXiv pre-print server (2020).
[117] H. Zhou, H. Cao, L. Matyunina, M. Shelby, L. Cassels, J.F. McDonald, J. Skolnick, MEDICASCY: A Machine Learning Approach for Predicting Small-Molecule Drug Side Effects, Indications, Efficacy, and Modes of Action, Molecular Pharmaceutics 17(5) (2020) 1558-1574.
[118] R.C. Braga, V.M. Alves, M.F.B. Silva, E. Muratov, D. Fourches, L.M. Lião, A. Tropsha, C.H. Andrade, Pred-hERG: A Novel web-Accessible Computational Tool for Predicting Cardiac Toxicity, Molecular Informatics 34(10) (2015) 698-701.

[119] L. Pu, M. Naderi, T. Liu, H.-C. Wu, S. Mukhopadhyay, M. Brylinski, eToxPred: a machine learning-based approach to estimate the toxicity of drug candidates, BMC Pharmacology and Toxicology 20(1) (2019) 2.
[120] C. Huang, R. Mezencev, J.F. McDonald, F. Vannberg, Open source machine-learning algorithms for the prediction of optimal cancer drug therapies, PLoS One 12(10) (2017).
[121] E. Wilhelm, S. Siby, Y. Zhou, X.J.S. Ashok, M. Jayasuriya, S. Foong, J. Kee, K.L. Wood, N.O. Tippenhauer, Wearable Environmental Sensors and Infrastructure for Mobile Large-Scale Urban Deployment, IEEE Sensors Journal 16(22) (2016) 8111-8123.
[122] C.A. Oroza, Z. Zhang, T. Watteyne, S.D. Glaser, A Machine-Learning-Based Connectivity Model for Complex Terrain Large-Scale Low-Power Wireless Deployments, IEEE Transactions on Cognitive Communications and Networking 3(4) (2017) 576-584.
[123] J. Wiens, S. Saria, M. Sendak, M. Ghassemi, V.X. Liu, F. Doshi-Velez, K. Jung, K. Heller, D. Kale, M. Saeed, P.N. Ossorio, S. Thadaney-Israni, A. Goldenberg, Do no harm: a roadmap for responsible machine learning for health care, Nature Medicine 25(9) (2019) 1337-1340.
[124] D. Harnie, M. Saey, A.E. Vapirev, J.K. Wegner, A. Gedich, M. Steijaert, H. Ceulemans, R. Wuyts, W. De Meuter, Scaling machine learning for target prediction in drug discovery using Apache Spark, Future Generation Computer Systems 67 (2017) 409-417.
[125] S. Jackson, M. Yaqub, C.-X. Li, The Agile Deployment of Machine Learning Models in Healthcare, Frontiers in Big Data 1(7) (2019).
[126] D. Sculley, G. Holt, D. Golovin, E. Davydov, T. Phillips, D. Ebner, V. Chaudhary, M. Young, J.-F. Crespo, D. Dennison, Hidden technical debt in machine learning systems, Advances in neural information processing systems, 2015, pp. 2503-2511.
[127] I. Flaounas, Beyond the technical challenges for deploying Machine Learning solutions in a software company, arXiv preprint arXiv:1708.02363 (2017).
[128] B. Ding, M. Wang, X. Wang, J. Yu, G. Sun, Electrospun nanomaterials for ultrasensitive sensors, Materials Today 13(11) (2010) 16-27.
[129] M. Premasudha, S.R. Bhumi Reddy, Y.-J. Lee, B.B. Panigrahi, K.-K. Cho, S.R. Nagireddy Gari, Using artificial neural networks to model and interpret electrospun polysaccharide (Hylon VII starch) nanofiber diameter, Journal of Applied Polymer Science 138(11) (2021) 50014.
[130] L. Kong, G.R. Ziegler, Quantitative relationship between electrospinning parameters and starch fiber diameter, Carbohydrate Polymers 92(2) (2013) 1416-1422.
[131] S. Kalantary, A. Jahani, R. Pourbabaki, Z. Beigzadeh, Application of ANN modeling techniques in the prediction of the diameter of PCL/gelatin nanofibers in environmental and medical studies, RSC Advances 9(43) (2019) 24858-24874.
[132] S. Kalantary, A. Jahani, R. Jahani, MLR and ANN Approaches for Prediction of Synthetic/Natural Nanofibers Diameter in the Environmental and Medical Applications, Scientific Reports 10(1) (2020) 8117.
[133] T. Khatti, H. Naderi-Manesh, S.M. Kalantar, Application of ANN and RSM techniques for modeling electrospinning process of polycaprolactone, Neural Computing and Applications 31(1) (2019) 239-248.
[134] P.I. Siafaka, P. Barmbalexis, D.N. Bikiaris, Novel electrospun nanofibrous matrices prepared from poly(lactic acid)/poly(butylene adipate) blends for controlled release formulations of an anti-rheumatoid agent, European Journal of Pharmaceutical Sciences 88 (2016) 12-25.

[135] K. Nasouri, Novel estimation of morphological behavior of electrospun nanofibers with artificial intelligence system (AIS), Polymer Testing 69 (2018) 499-507.
[136] R. Faridi-Majidi, H. Ziyadi, N. Naderi, A. Amani, Use of artificial neural networks to determine parameters controlling the nanofibers diameter in electrospinning of nylon-6,6, Journal of Applied Polymer Science 124(2) (2012) 1589-1597.
[137] E. Mirzaei, A. Amani, S. Sarkar, R. Saber, D. Mohammadyani, R. Faridi-Majidi, Artificial neural networks modeling of electrospinning of polyethylene oxide from aqueous acid acetic solution, Journal of Applied Polymer Science 125(3) (2012) 1910-1921.
[138] A.K. Maurya, P.L. Narayana, A.G. Bhavani, H. Jae-Keun, J.-T. Yeom, N.S. Reddy, Modeling the relationship between electrospinning process parameters and ferrofluid/polyvinyl alcohol magnetic nanofiber diameter by artificial neural networks, Journal of Electrostatics 104 (2020) 103425.
[139] A. Reisi-Dehkordi, R. Eslami-Farsani, Prediction of High Performance Fibers Strength Using Back Propagation Neural Network, Journal of Macromolecular Science, Part A 52(8) (2015) 642-647.
[140] E. Vatankhah, D. Semnani, M.P. Prabhakaran, M. Tadayon, S. Razavi, S. Ramakrishna, Artificial neural network for modeling the elastic modulus of electrospun polycaprolactone/gelatin scaffolds, Acta Biomaterialia 10(2) (2014) 709-721.
[141] C. Ieracitano, A. Paviglianiti, M. Campolo, A. Hussain, E. Pasero, F.C. Morabito, A novel automatic classification system based on hybrid unsupervised and supervised machine learning for electrospun nanofibers, IEEE/CAA Journal of Automatica Sinica 8(1) (2021) 64-76.
[142] A. Ziaee, S. O'Dea, A. Howard-Hildige, L. Padrela, C. Potter, J. Iqbal, A.B. Albadarin, G. Walker, E.J. O'Reilly, Amorphous solid dispersion of ibuprofen: A comparative study on the effect of solution based techniques, International Journal of Pharmaceutics 572 (2019) 118816.
[143] A.K. Ball, R. Das, S.S. Roy, D.R. Kisku, N.C. Murmu, Modeling of EHD inkjet printing performance using soft computing-based approaches, Soft Computing 24(1) (2020) 571-589.
[144] N.M. Mahmoodi, M. Oveisi, A. Taghizadeh, M. Taghizadeh, Synthesis of pearl necklace-like ZIF-8@chitosan/PVA nanofiber with synergistic effect for recycling aqueous dye removal, Carbohydrate Polymers 227 (2020) 115364.
[145] H. Jamalabadi, A. Mani-Varnosfaderani, N. Alizadeh, Detection of alkyl amine vapors using PPy-ZnO hybrid nanocomposite sensor array and artificial neural network, Sensors and Actuators A: Physical 280 (2018) 228-237.
[146] G. Ciaburro, G. Iannace, J. Passaro, A. Bifulco, D. Marano, M. Guida, F. Marulo, F. Branda, Artificial neural network-based models for predicting the sound absorption coefficient of electrospun poly(vinyl pyrrolidone)/silica composite, Applied Acoustics 169 (2020) 107472.
[147] E. Hosaini-Alvand, H. Mirshekar, M. Taghi Khorasani, M. Parvazinia, A. Joorabloo, Fabricating and robust artificial neural network modeling nanoscale polyurethane fiber using electrospinning method, Journal of Applied Polymer Science 134(30) (2017) 45116.
[148] V. Nourani, M. Sayyah Fard, Sensitivity analysis of the artificial neural network outputs in simulation of the evaporation process at different climatologic regimes, Advances in Engineering Software 47(1) (2012) 127-146.
[149] Y. Yin, J. Xiong, Finite element analysis of electrospun nanofibrous mats under biaxial tension, Nanomaterials 8(5) (2018) 348.

[150] S. Zhao, X. Zhao, S. Dong, J. Yu, G. Pan, Y. Zhang, J. Zhao, W. Cui, A hierarchical, stretchable and stiff fibrous biotemplate engineered using stagger-electrospinning for augmentation of rotator cuff tendon-healing, Journal of Materials Chemistry B 3(6) (2015) 990-1000.
[151] U.E. Illangakoon, H. Gill, G.C. Shearman, M. Parhizkar, S. Mahalingam, N.P. Chatterton, G.R. Williams, Fast dissolving paracetamol/caffeine nanofibers prepared by electrospinning, International Journal of Pharmaceutics 477(1) (2014) 369-379.
[152] L. Chen, G. Pilania, R. Batra, T.D. Huan, C. Kim, C. Kuenneth, R. Ramprasad, Polymer informatics: Current status and critical next steps, Materials Science and Engineering: R: Reports 144 (2021) 100595.
[153] F. Yu, T. Lu, B. Han, C. Xue, A quantitative study of aggregation behaviour and integrity of spray-dried microcapsules using three deep convolutional neural networks with transfer learning, Journal of Food Engineering 300 (2021) 110515.
[154] A. Krizhevsky, I. Sutskever, G.E. Hinton, ImageNet classification with deep convolutional neural networks, Commun. ACM 60(6) (2017) 84–90.
[155] S.J. Kim, J.W. Lee, D.H. Kwon, S.K. Han, Gamma Function Based Signal Compensation for Transmission Distance Tolerant Multilevel Modulation in Optical Camera Communication, IEEE Photonics Journal 10(5) (2018) 1-7.
[156] J. Yao, X. Chen, Y. Zhou, H. Miao, J. Chen, Phase error elimination considering gamma nonlinearity, system vibration, and noise for fringe projection profilometry, Optical Engineering 53(9) (2014) 094102.
[157] C. Cogswell, N. Smith, K. Larkin, P. Hariharan, Quantitative DIC microscopy using a geometric phase shifter, SPIE1997.
[158] L. Ren, J. Lu, J. Feng, J. Zhou, Uniform and Variational Deep Learning for RGB-D Object Recognition and Person Re-Identification, IEEE Transactions on Image Processing 28(10) (2019) 4970-4983.
[159] A. Akbarinia, C.A. Parraga, Colour Constancy Beyond the Classical Receptive Field, IEEE Transactions on Pattern Analysis and Machine Intelligence 40(9) (2018) 2081-2094.
[160] C.K. Groschner, C. Choi, M. Scott, Methodologies for successful segmentation of HRTEM Images via neural network, arXiv preprint arXiv:2001.05022 (2020).
[161] J. Sun, L. Jing, X. Fan, X. Gao, Y. C.Liang, Electrohydrodynamic printing process monitoring by microscopic image identification, 2019 5(1) (2019).
[162] M. Ma, Y. Zou, Z. Huang, Deep learning-based automated morphology classification of electrospun ultrafine fibers from M44 element image of muller matrix, Optik 206 (2020) 164261.
[163] G. Ivosev, L. Burton, R. Bonner, Dimensionality Reduction and Visualization in Principal Component Analysis, Analytical Chemistry 80(13) (2008) 4933-4944.
[164] D. Mladenić, Feature Selection for Dimensionality Reduction, Springer Berlin Heidelberg, Berlin, Heidelberg, 2006, pp. 84-102.
[165] A. Malhi, R.X. Gao, PCA-based feature selection scheme for machine defect classification, IEEE Transactions on Instrumentation and Measurement 53(6) (2004) 1517-1525.
[166] K. Han, Y. Wang, C. Zhang, C. Li, C. Xu, Autoencoder Inspired Unsupervised Feature Selection, 2018 IEEE International Conference on Acoustics, Speech and Signal Processing (ICASSP), 2018, pp. 2941-2945.

[167] V.L. Cao, M. Nicolau, J. McDermott, A Hybrid Autoencoder and Density Estimation Model for Anomaly Detection, Springer International Publishing, Cham, 2016, pp. 717-726.
[168] J. Ma, S.H. Fong, Y. Luo, C.J. Bakkenist, J.P. Shen, S. Mourragui, L.F.A. Wessels, M. Hafner, R. Sharan, J. Peng, T. Ideker, Few-shot learning creates predictive models of drug response that translate from high-throughput screens to individual patients, Nature Cancer 2(2) (2021) 233-244.
[169] K. Ni, X. Yin, A.F. Laguna, S. Joshi, S. Dünkel, M. Trentzsch, J. Müller, S. Beyer, M. Niemier, X.S. Hu, S. Datta, Ferroelectric ternary content-addressable memory for one-shot learning, Nature Electronics 2(11) (2019) 521-529.
[170] Y. Zhu, Z. Wu, W.D. Hartley, J.M. Sietins, C.B. Williams, H.Z. Yu, Unraveling pore evolution in post-processing of binder jetting materials: X-ray computed tomography, computer vision, and machine learning, Additive Manufacturing 34 (2020) 101183.
[171] J.P. Horwath, D.N. Zakharov, R. Mégret, E.A. Stach, Understanding important features of deep learning models for segmentation of high-resolution transmission electron microscopy images, npj Computational Materials 6(1) (2020) 108.
[172] N. Scoutaris, S.A. Ross, D. Douroumis, 3D Printed “Starmix” Drug Loaded Dosage Forms for Paediatric Applications, Pharmaceutical Research 35(2) (2018) 34.
[173] M. Elbadawi, L.E. McCoubrey, F.K.H. Gavins, J.J. Ong, A. Goyanes, S. Gaisford, A.W. Basit, Harnessing artificial intelligence for the next generation of 3D printed medicines, Advanced Drug Delivery Reviews 175 (2021) 113805.